Optimal Control of Pitch and Rotational Velocity for a Cyclorotor Wave Energy Device

Andrei Ermakov, Alice Marie, and John V. Ringwood, *Senior Member, IEEE*

***Abstract*—The development of optimal control strategies for cyclorotor wave energy converters (WECs) is at an early stage. In this paper, we present new methods and solutions for optimal pitch and/or rotational velocity control strategies for different configurations of cyclorotor-based WECs, in both monochromatic and panchromatic waves. The cyclorotor is modelled with the use of an approximate two-dimensional mathematical model, where hydrofoils are approximated as point source vortices in potential waves. The goal of the developed control strategy is to determine the optimal velocity profile, and/or pitch angle variations, for maximum energy conversion, in terms of generated mechanical shaft power. The solutions, obtained with the use of spectral methods, show a clear benefit in using a variable velocity for cyclorotors with either one or two hydrofoils, in monochromatic waves, with a typical increase in energy capture of 30-40%, while the optimal pitching did not significantly increase the value of the absorbed wave energy. We also present control results for panchromatic waves, assuming all the properties of incoming wave packages, within a 10 s time interval, are known. The obtained solutions have shown significant benefit in joint optimal pitch and velocity control, especially in the case of panchromatic waves. It has been also shown that successful implementation of cyclorotor control strategies requires optimal configuration of the static characteristics of the cyclorotor. In conclusion, we discuss the optimal control benefits and highlight problems which must be solved for further successful development of these control strategies.**

***Index Terms*—Cyclorotor, LiftWEC, lift-based wave energy converter, optimal control, wave energy converter.**

I. Introduction

A. The Problem of Optimal Optimal Control for Cyclorotor-Based Wave Energy Converters

ALTHOUGH there is significant wave energy available world-wide, after almost 50 years of research and development no commercially successful technology has been developed. One of the reasons is the limited focus of the research in this area. None of the traditional WECs, which harness buoyancy or diffraction wave forces have shown themselves to be commercially viable. This creates motivation to develop new principles for wave energy extraction. Recently, a lift-based wave energy converter (Fig. 1) that utilises lift force generated on hydrofoils due to their interaction with wave induced circular motion of water particles, started to attract more and more attention from various research groups [1], [2]. Cyclorotor based WECs have a number of appealing characteristics, including the potential for unidirectional rotation, simplified power take-off, and reduction of wave loads by adjusting pitch angles, increasing survivability. However, as it has been shown in [3]–[6], the performance of the cyclorotor requires real-time control (especially in panchromatic seas). The reviews of cyclorotor-based WECs [6]–[8] have identified the variation of the rotational rate and hydrofoil pitch angle as the most advanced actuators. However, the optimal control strategies, the best real-time actuators, and appropriate performance metrics, need to be identified. At this moment, only three concepts and their control methods have been presented for cyclorotor-based WECs.

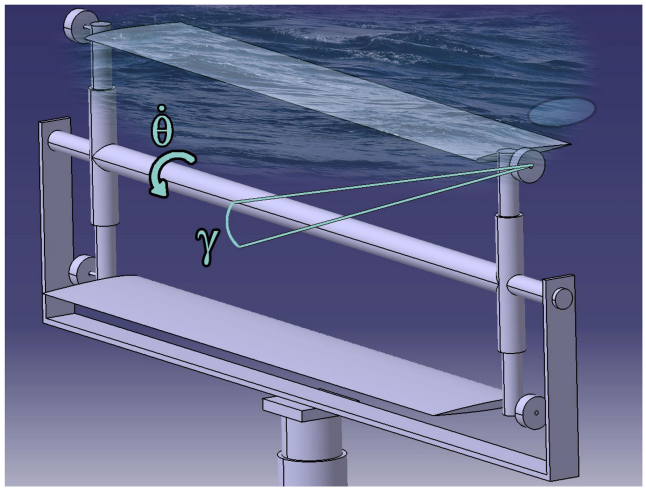

Fig. 1. The concept of the cyclorotor proposed in [2], [7], showing the real-time manipulated variables $\dot{\theta}$ and γ.

The first cyclorotor concept, a single 'Rotating Wing,' was studied in the wave tank of the Maritime Research Institute, in the Netherlands by Hermans *et al.* [9] in 1990. It was shown analytically, and then experimentally, that the rotor could extract wave energy by canceling incoming waves [9], [10]. The authors proposed that the phase and rotational rate should be maintained in agreement with the incoming wave frequency as the operational control strategy.

Manuscript received December 6, 2021; revised March 11, 2022; accepted April 9, 2022. Date of publication April 19, 2022; date of current version June 21, 2022. This work was supported by the European Union's Horizon 2020 Research and Innovation Programme under Grant 851885. Paper no. TSTE-01224-2021. *(Corresponding author: Andrei Ermakov.)*

Andrei Ermakov and John V. Ringwood are with the Centre for Ocean Energy Research, Maynooth University, W23 F2K8 Maynooth, Kildare, Ireland (e-mail: andrei.ermakov@mu.ie; john.ringwood@mu.ie).

Alice Marie is with the Ecole Centrale de Nantes, 44300 Nantes, France (e-mail: alice.marie@eleves.ec-nantes.fr).

Color versions of one or more figures in this article are available at https://doi.org/10.1109/TSTE.2022.3168508.

Digital Object Identifier 10.1109/TSTE.2022.3168508

This work is licensed under a Creative Commons Attribution 4.0 License. For more information, see https://creativecommons.org/licenses/by/4.0/

The second, and the most advanced, feedback control strategy for a cyclorotor with two hydrofoils, the 'Cycloidal Wave Energy Converter' (CycWEC) was developed by the Atargis Energy Corporation [1], [6], [11]. The developed wave cancellation control strategy uses the idea of wave *generation* similar to the incoming wave, but with the opposite phase. The proposed control system should select the corresponding constant rotational rate to satisfy the predominant incoming wave period and maintain optimal hydrofoil pitch angles to create the necessary level of circulation corresponding to a generated wave amplitude. The efficiency of this control strategy is generally evaluated as the difference between power of the incoming and transmitted waves, which can be estimated by upwave and downwave far-field free surface perturbation. The proposed optimal control algorithm was tested in numerical simulations [6], [11], for a 1:300 scale prototype in a 2D wave tunnel of the US Air Force Academy [12], [13], and as a 1:10 scale model in a 3D wave tank at the Texas A&M Offshore Technology Research Center [14], [15]. The CycWEC energy production, in terms of mean annual absorbed power, is calculated at 619 kW for the US West Coast at Humboldt Bay [6]. This value is 40% higher than annual mean power output of the best traditional WECs, which shows considerable promise for cyclorotor-based wave energy technology.

Inspired by the first presentations of CycWEC, Nik Scharmann [16] dedicated his PhD study to this new WEC technology. Scharmann developed his concept of 'The Wave Hydromechanical Rotary Energy Converter' (WH-WEC), - a cyclorotor with four hydrofoils, and contributed valuable results by setting up physical experiments in the Hamburg Ship Model Basin (Germany), with complementary computational simulation in Ansys Fluid and OpenFOAM. The robust control strategy proposed for the WH-WEC in [16] is also based on the maintenance of the wave phase fixed optimal constant rotational rate. The author estimated the rated power for a cyclorotor at the European Marine Energy Centre (EMEC) test site as $\approx$ 800 kW, comparable with wind turbine technology.

The promising power production assessments presented in these previous research, and general lack of definitive knowledge about this new technology, motivated the inception of a new Horizon 2020 project dedicated to the development of a Lift-Based Wave Energy Converter (LiftWEC) [2]. The members of the consortium selected a rotor with two hydrofoils as a foundation for further development of the LiftWEC prototype [17]–[19]. As members of the LiftWEC consortium, the authors derive new optimal pitch and rotational rate control strategies for a cyclorotor with two hydrofoils. The presented strategies can potentially significantly increase the cyclorotor performance, in terms of the generated shaft power.

B. Paper Structure, Innovations and Limitations

In this article we develop spectral methods for the optimal control of a cyclorotor WEC. We propose some new possibilities for optimal control algorithms for a cyclorotor, with one or two hydrofoils (Fig. 1). The control strategies are based on variations in hydrofoil pitch angles and rotational rate, as manipulated variables, for various monochromatic and panchromatic waves types.

The optimisation of the variable rotational rate and hydrofoils pitch angles has been conducted only in terms of pure mechanical power capture. The inclusion of an electrical generator and other PTO components may yield different results [21]. The rotation rate, in general, is directly measurable. However, a position or velocity servo control loop (with generator torque as the manipulated variable) is envisaged in a real-world setting. For the purpose of this initial control investigation, we assume that the velocity is directly specifiable.

The developed optimal control strategy can be considered as an alternative to the traditional approach which has been proposed and developed by the Atargis energy corporation [6], [11]. Our goal is to directly maximise mechanical shaft power rather than maximisation of the difference between the incoming and transmitted wave. The difference in the shaft power and wave cancellation metric is primarily due to the fact that, when maximising shaft power, tangential force needs to be maximised while, for wave cancellation circulation Γ needs to be optimised [6], [22].

In Section II, we briefly present the two dimensional analytical point-source model of a cyclorotor-based WEC, which is used as a basis for optimal model-based control design [22]–[24]. Section II also describes the numerical methods used for the optimisation problem solution, and the constraints on rotational rate, mechanical torque and pitch values. In Section III, we present periodic control solutions for rotational rate and hydrofoil pitch angle, for cyclorotor-based WECs with one or two hydrofoils, and analyse the convergence of the developed spectral approaches. In Section IV, we present the application of the developed and analysed spectral methods to the optimal control problem for a cyclorotor-based WEC in *panchromatic* waves. In conclusion (Section V), we review the obtained results and discuss the perspectives and problems of the developed optimal control methods

II. Mathematical Formulation of the Optimal Control Problem

We consider the 2-D mathematical model of a cyclorotor, the hydrofoils of which interact with potential waves. We model the hydrofoils using a point-source representation [22]–[24], with the corresponding equations validated against experimental results obtained by previous research [9], [11], [14] in terms of waves radiated by a rotor. The model also has been validated [25] in terms of tangential and radial forces against experimental results obtained in the Hamburg Ship Model Basin, (Germany) [16] and against the recent experimental results of the LiftWEC project [2] which were obtained in the wave flume of Ecole Centrale de Nantes, (France) [26], [27].

In the point source model, it is assumed that the lift, drag and tangential forces are caused by the interaction of the rotation of hydrofoil i with an overall relative velocity $\hat{\mathbf{V}}_\mathbf{i}$, representing the vector difference between the wave induced fluid velocity $\mathbf{V}_{\mathbf{W}_\mathbf{i}}$ and the cyclorotor rotational velocity $\mathbf{V}_{\mathbf{R}_\mathbf{i}}$, plus the sum of the wakes left by the moving foils $\mathbf{V}_{\mathbf{HW}}$, and the instantaneous

radiation from the other foils $\mathbf{V_{HM}}$ as:

$$\hat{\mathbf{V}}_\mathbf{i} = \mathbf{V}_{\mathbf{W}_\mathbf{i}} - \mathbf{V}_{\mathbf{R}_\mathbf{i}} + \mathbf{V}_{\mathbf{HW}\mathbf{i}} + \mathbf{V}_{\mathbf{HM}\mathbf{j}} + \mathbf{V}_{\mathbf{HW}\mathbf{j}} \quad (1)$$

The rotational velocity components $\mathbf{V_R}$ for foil i can be found as the partial time derivatives of the hydrofoil positions (x_i, y_i) where:

$$x_i = R\cos(\theta(t) + \pi(i-1)), \quad y_i = y_0 - R\sin(\theta(t) + \pi(i-1)) \quad (2)$$

where $\theta(t)$ is the position of the hydrofoil in polar coordinates, R is the radius and y_0 is the submergence of the rotor's centre.

The velocity components $\mathbf{V_W}$ of the wave-induced water particle movements can be found as the partial derivative of the potential, using the corresponding coordinate. For example, for the case of the Airy potential, the velocity components can be found as a gradient:

$$\Phi_W = \frac{Hg}{2\omega} e^{ky} \sin(kx - \omega t) \quad (3)$$

$$\mathbf{V_W} = \nabla \Phi_W \quad (4)$$

where H is the height, ω is the frequency and k is the number of the incoming wave, with g being gravitational acceleration. The velocity components of the waves radiated by the moving point source can be described by the following formula:

$$\mathbf{V_H} = \frac{\partial \mathcal{F}(z,t)}{\partial z} = (V_H)_x - \mathbb{i}\,(V_H)_y \quad (5)$$

which can be separated into the instantaneous radiated waves $\mathbf{V_{HM}}$, and wakes $\mathbf{V_{HW}}$, which are left in the hydrofoil's path:

$$\mathbf{V_H} = \mathbf{V_{HM}} + \mathbf{V_{HW}} \quad (6)$$

The waves generated by hydrofoils are described by the use of the complex potential, derived in [22], [23], as:

$$\mathcal{F}(z,t) = \frac{\Gamma(t)}{2\pi\mathbb{i}} Log\left[\frac{z - c(t)}{z - \tilde{c}(t)}\right] - \frac{2\mathbb{i}\sqrt{g}}{\pi} \int_0^t \frac{\Gamma(\tau)}{\sqrt{\mathbb{i}(z - \tilde{c}(\tau))}} D\left[\frac{\sqrt{g}(t-\tau)}{2\sqrt{\mathbb{i}(z - \tilde{c}(\tau))}}\right] d\tau \quad (7)$$

where $z = x + \mathbb{i}y$ is the coordinate on the complex plain, $c(t) = x(t) + \mathbb{i}y(t)$ is the position of the hydrofoil, $\tilde{c}(t)$ is the complex conjugate of $c(t)$, $\Gamma(t)$ - is the circulation of the point-source vortex and $D(x)$ is the Dawson function [28]:

$$D(x) = e^{-x^2} \int_0^x e^{y^2} dy. \quad (8)$$

The velocity potential Φ_H of the waves radiated by the moving foils can be found from the following relation:

$$\Phi_H(x,y) = Re[\mathcal{F}(z,t)] \quad (9)$$

The generated on the hydrofoils tangential forces F_T depend on the lift and drag coefficients $C_L(\alpha)$ and $C_D(\alpha)$, respectively, the chord length of the hydrofoil C, the water density ρ, and the overall relative to hydrofoil fluid velocity $\hat{\mathbf{V}}$ at the current particular hydrofoil position (x_i, y_i):

$$F_T = \frac{1}{2}\rho(C_L(\alpha)\sin(\alpha - \gamma) - C_D(\alpha)\cos(\alpha - \gamma))|\hat{V}|^2 C \quad (10)$$

where γ is the optimal *variable* hydrofoil pitch angle and α is the attack angle. The circulation Γ can be found from the Kutta–Joukowski theorem [29] as:

$$\Gamma = \frac{1}{2} C_L(\alpha)\,|\hat{V}|\,C \quad (11)$$

Cyclorotor WECs extracts wave energy from the system via the torque $\mathcal{T}$ on the rotor/generator shaft. The rotational rate $\dot{\theta}(t)$ can be controlled by manipulating the generator torque $\mathcal{T}_{gen}$ and/or the hydrofoil pitch angles γ_i.

$$\mathcal{T} = \left(F_{T_1}[\theta, \dot{\theta}, \gamma_1] + F_{T_2}[\theta, \dot{\theta}, \gamma_2]\right) R - I\ddot{\theta}(t) \quad (12)$$

where I is the moment of inertia of the cyclorotor (including any attached generator), and $\ddot{\theta}(t)$ is the rotational acceleration. Optimisation of energy production, which is the control objective, is solved in terms of the mean mechanical power, which is determined as:

$$P_{Shaft} = \frac{1}{T}\int_0^T \mathcal{T}(t)\dot{\theta}(t)dt \quad (13)$$

We assume that the power is linearly proportional to the shaft span of the rotor and assess it in [kW/m]. The detailed explanation of the control problem and relationships between the equations is presented as a block diagram in Fig. 2.

In the case of a cyclorotor WEC, which starts rotation in monochromatic waves with the same phase and rotational rate, all hydrodynamic and mechanical processes became periodic after $K \sim 8$ rotational periods. Thus, the mechanical energy which can be generated during one stable period in monochromatic waves, in terms of shaft power, can be evaluated by substantiation of the expression for shaft torque (12) into the functional (13):

$$Max \quad \frac{R}{T}\int_{T_K}^{T_{K+1}} (F_{T_1} + F_{T_2})\,\dot{\theta}(t)dt \quad (14)$$

The influence of the moment of inertia I in (12) is canceled during the integration (13) because we presume the periodic solution for variable rotational rate on the selected time interval $\dot{\theta}(T_{K+1}) = \dot{\theta}(T_K)$.

We search for periodic solutions that describe the rotation of the cyclorotor in monochromatic waves, with a variable rotational rate $\dot{\theta}(t)$, or hydrofoil pitch angles values $\gamma_i(t)$, within the wave period T, which increase energy absorption in terms of the shaft power metric in (14). Our approach is inspired by pseudo-spectral [30] and moment-based [31] methods, originally developed for more general categories of WECs. Then, the rotor position $\theta(t)$, within the rotational period, can be presented in the form of a Fourier series with the period equivalent to monochromatic waves period T, requiring the solution for the $a_{mv,i}$ and $b_{mv,i}$ coefficients and determination of the optimal number of harmonics m required for the solution convergence:

$$\theta(t) = \omega\, t + \sum_{i=1}^{m} a_{mv,i}\cos\left(\frac{2\pi\, t}{T} i\right) + b_{mv,i}\sin\left(\frac{2\pi\, t}{T} i\right) \quad (15)$$

where ω is the frequency of the incoming monochromatic wave. The rotational rate $\dot{\theta}$ can be obtain by differentiation of the series.

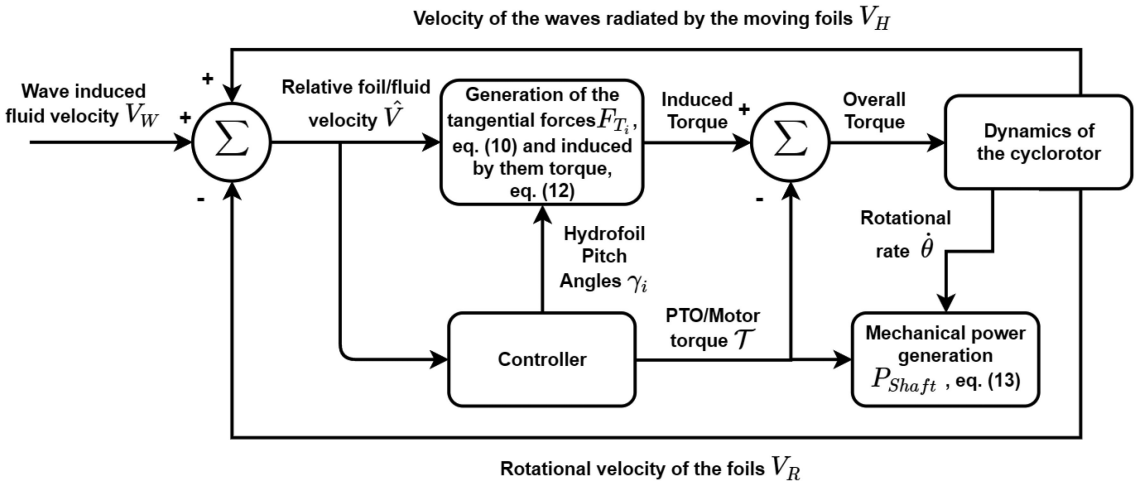

Fig. 2. Block diagram showing the control structure and relationships between the model equations.

A similar spectral approach can be applied to the optimal pitch control problem. Thus, the position of the pitch angle $\gamma(t)$ of a cyclorotor with a single hydrofoil within the rotational period can be presented in the following form:

$$\gamma(t) = \gamma_0 + \sum_{i=1}^{m} a_{mp,i} \cos\left(\frac{2\pi\, t}{T} i\right) + b_{mp,i} \sin\left(\frac{2\pi\, t}{T} i\right) \tag{16}$$

where γ_0 is the optimal constant pitch angle for the incoming monochromatic wave, $a_{mp,i}$ and $b_{mp,i}$ are series coefficients for variable pitch. The series (15) and (16) also allow us to obtain the optimal position, rotational rate and pitch angles at the beginning and the end of the considered wave period T.

In the case of panchromatic waves, we cannot use periodic solution (15), (16). We must also take into account the influence of the moment of inertia I of the rotor (12), because $\dot{\theta}(T_{K+1}) \neq \dot{\theta}(T_K)$. The optimisation also must start after the moment T_0 when the complex (caused by rotation) velocity field has formed in the vicinity of the rotor. Then, for the case of panchromatic waves, the shaft power functional has the following form:

$$Max \quad \frac{1}{(T - T_0)} \int_{T_0}^{T} \left((F_{T_1} + F_{T_2})R - I\ddot{\theta}(t)\right) \dot{\theta}(t) dt \tag{17}$$

We also apply the Fourier series with a phase shift for the solution of the optimal variable rotational rate in panchromatic waves:

$$\theta(t) = \dot{\theta}_0 t + \sum_{i=1}^{m} a_{pv,i} \cos\left(\frac{2\pi\, t}{T_{ext}} i + c_{pv,i}\right) + b_{pv,i} \sin\left(\frac{2\pi\, t}{T_{ext}} i + d_{pv,i}\right) \tag{18}$$

where $\dot{\theta}_0$ is the optimal constant rotational rate for the incoming panchromatic waves, $a_{pv,i}$ and $b_{pv,i}$ are series coefficients, T_{ext} is the extended time interval which is selected at two times greater then the interval on which we consider the energy generation $[T_0, T]$. The condition ensures that, at the start of the power generation interval, the hydrofoils have an optimal initial position, rotational rate, and the most favourable wake field has been formed. It also permits a non-periodic solution, over the limited solution domain. The additional coefficients shift $c_{pv,i}$ and $d_{pv,i}$ allow us to achieve faster convergence for smaller m values. Even though, the additional coefficients increase the complexity of the optimisation problem, they significantly speed up calculations provide some immunity to local minimum. A similar series is used to estimate the benefits of application of optimal pitch control in panchromatic waves:

$$\gamma(t) = \gamma_0 + \sum_{i=1}^{m} a_{pp,i} \cos\left(\frac{2\pi\, t}{T_{ext}} i + c_{pp,i}\right) + b_{pp,i} \sin\left(\frac{2\pi\, t}{T_{ext}} i + d_{pp,i}\right) \tag{19}$$

where γ_0 is the optimal constant pitch angle for the incoming panchromatic waves, $a_{pp,i}$, $b_{pp,i}$, $c_{pp,i}$ and $d_{pp,i}$ are series coefficients.

The cyclorotor-based WEC is simulated with the use of a bespoke mathematical model which has an integro-differential equation form (1)–(12), simulated in Python [32]. The control problem is non-convex due to the high non-linearity of the model equations. A closed-form expression for ($\dot{\theta}_0$, γ_0, a_i, b_i, c_i, d_i) cannot be obtained; rather, purely numerical solution methods for the presented non-linear non-convex problem are used. The control optimisation problem is solved with the use of a finite difference numerical method [33] for the discretised system equations and global optimisation methods, implemented in Python [32], are employed. The authors used, and compared, two different global optimisation approaches (simplicial homology global optimisation [34] and differential evolution [35]) in order to increase the probability of obtaining the global maximum.

We use the trapezoidal method to integrate the functionals of (14) and (17). The simulated time is separated into n intervals $\Delta t_i = \{t_i, t_{i+1}\}$, $0 \leq i \leq n$. The values of the pitch angle γ_i, hydrofoil position θ_i, rotation rate $\dot{\theta}_i$ and acceleration $\ddot{\theta}_i$ at time step t_i can be obtained from (15), (16) or (18), (19), for monochromatic and panchromatic waves, respectively. The

numerical integration transforms the functionals (14), (17) into a complex nonlinear algebraic function U, which needs to be maximised using the coefficients $\dot{\theta}_0$, γ_0, $a_{i/j}, b_{i/j}, c_{i/j}, d_{i/j}$:

$$\underset{\dot{\theta}_0,\gamma_0,a_{i/j},b_{i/j},c_{i/j},d_{i/j}}{Max} U\left[\theta(\dot{\theta}_0,a_i,b_i,c_i,d_i),\gamma(\gamma_0,a_j,b_j,c_j,d_j)\right] \tag{20}$$

The solutions of (14) and (17) are subject to additional physical and engineering constraints. Thus, the value of the torque $\mathcal{T}$ should be limited according to device characteristics $\mathcal{T}_{PTO} < \mathcal{T} < \mathcal{T}_{Motor}$, where $\mathcal{T}_{Motor}$ is the maximum torque which can be supplied by a motor, and $\mathcal{T}_{PTO}$ is the maximum torque which can be absorbed by a power take off (PTO). Limitations on the torque derivative $\mathcal{T}'_{PTO} < \mathcal{T}' < \mathcal{T}'_{Motor}$ recognise the speed limitation in switching from generating to motoring mode (and vice versa). Additional constraints also limit the rotational rate: $\dot{\theta}_{Min} < \dot{\theta} < \dot{\theta}_{Max}$, while excursions in pitch angle are limited to $|\gamma'(t)| < 5^o$ per second to avoid significant hydrodynamic pressure on hydrofoils. In addition, frequent changes of the rotational rate and hydrofoil pitch angles may create significant structural and generator loads, which could lead to fatigue of the system [25]. However, the effects of structural loading are beyond the scope of this study.

III. Optimal Real-Time Control in Monochromatic Waves

In this section, we present two forms of the optimal control solution for a cyclorotor in monochromatic waves, using shaft power as the performance metric. In the first case, we consider a variable rotational rate and optimal constant pitch angle and, in the second case, variable pitch and optimal constant rotational rate. Isolation of the real-time actuators in this way will provide guidance in terms of the relative merits of each actuator type. Control strategies are developed for cyclorotors with one or two hydrofoils, with geometric parameters selected from the CycWEC prototype proposed in [6]. The prototype has hydrofoils NACA0015, with chord length $C = 5$ m, operational radius $R = 6$ m and submergence depth $y_0 = -12$ m. The lift and drag coefficients are selected from [36] for symmetric hydrofoils NACA0015, for $Re = 10^7$. We consider asymmetric rotors, with two hydrofoils with opposite non-zero pitch angles, and assume their synchronous manipulation using the assumption from [6] where $\gamma_1 = -\gamma_2 = \gamma$. In order to provide sufficient control freedom, the constraint on the main shaft torque is selected as $|\mathcal{T}| < 2 \cdot 10^7\ Nm$. Variations in the rotation rate $\tilde{\omega} = \dot{\theta}/\omega$ are also limited to $1/2 < \tilde{\omega} < 2$, to satisfy realistic electrical machine capabilities.

We present results obtained for the described cyclorotor, operating in monochromatic waves, with wave period $T = 10$ s and wave height $H = 2$ m. It has been shown in [6], [19], that a cyclorotor which rotates with the constant rotational rate achieves maximum power production when the first hydrofoil has a -90^o phase shift relative to the wave crest (2)–(3). Thus the performance of the cyclorotor, with a single hydrofoils which rotates with a *constant* rotational rate $\dot{\theta} = \omega$, is calculated as $P_{Shaft} = 6.5$ kW/m, for *neutral* pitch positions $\gamma_1 = 0^o$, and at $P_{Shaft} = 13.1$ kW/m for the *optimal constant* pitch value

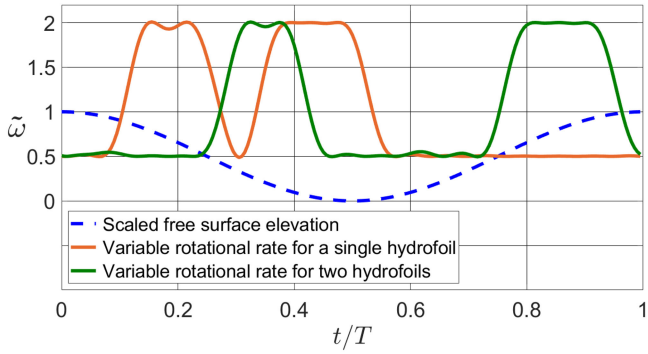

Fig. 3. The changes of the rotational rate within the wave period obtained for the case of the single hydrofoil (orange line, m = 20) and two hydrofoils (green line, m = 20), for optimal constant pitch angles. The scaled free surface elevation is presented for the reference.

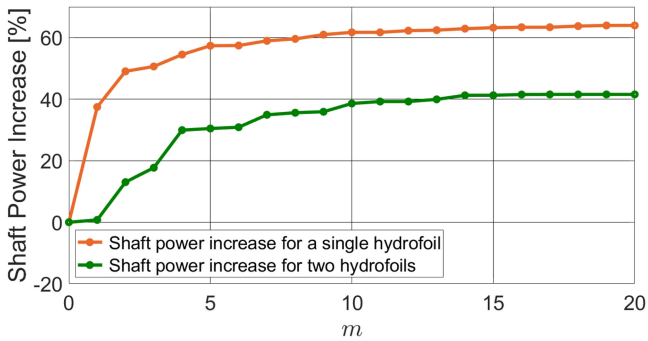

Fig. 4. The increase in the rotor's performance with the increase of the harmonics added to the solution for variable rotation rate and optimal constant pitch for cyclorotors with one and two hydrofoils.

$\gamma_1 = 9^o$. A similar significant increase in shaft power is obtained for the case of a twin-foil cyclorotor, which generates $P_{Shaft} = 12.8$ kW/m for $\gamma_i = 0$, and $P_{Shaft} = 24.1$ kW/m for the tuned optimal *constant* pitch values $\gamma_1 = -\gamma_2 = 11^o$. However, even this almost 100% power increase can be significantly exceeded, if *variable* rotational rate or pitch control strategies are applied.

The solutions for the case of variable rotational rate and optimal *constant* pitch angle, which are obtained with the use of spectral method (14), (15), are presented in Fig. 3. The convergence of the optimisation method used in the production of Fig. 4 was examined in terms of shaft power production (14).

It is clear from Fig. 4 that even the inclusion of four harmonics, $m = 4$ of (15), gives an increase in performance of 30% in the case of two hydrofoils, and 52% for the case of the single hydrofoil (Fig. 4), proving that maintaining a constant rotational rate is not optimal. Beyond m = 10, the inclusion of further harmonics does not increase the generated power value more than 5%. Of course, the additional constraints on the PTO/motor torque, acceleration/deceleration of the rotational rate and changes of the pitch angle per second also influence the early convergence of the obtained solutions. The irregular variations in the performance increase from step to step in Fig. 4 can be explained by the fact that we are using a mesh-based method in the calculations, while the solutions shown in Fig. 3) demonstrate that cyclorotors

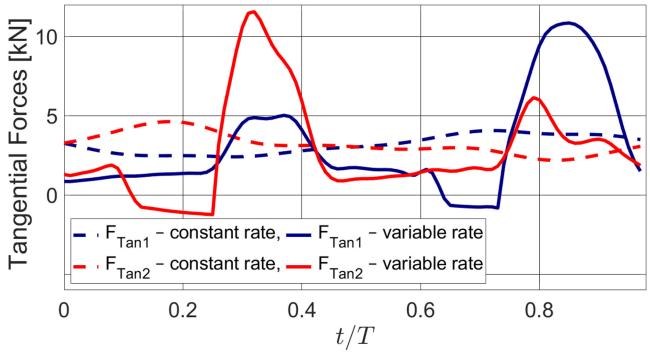

Fig. 5. Tangential forces for two hydrofoils for constant (dashed lines) and variable (solid lines) rotational rate.

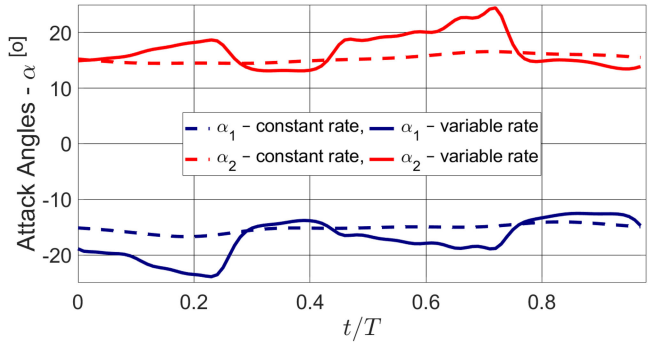

Fig. 6. Attack angles for two hydrofoils for constant rotational rate (dashed) and variable rotational rate (solid lines).

must switch between maximum and minimum possible rotational rates at different time moments, somewhat mimicing the action of latching control for conventional WECs [37].

Fig. 5 illustrates the corresponding changes in the tangential forces which act on two hydrofoils, with implementation of the variational rotation rate strategy. Such significant increases in the tangential forces values can be explained by the fact that they are proportional to the square of the overall relative hydrofoil/fluid velocity (see (10)). However, it is also important to maintain the optimal attack angle, at all times, to minimise drag losses. Fig. 6 illustrates that implementation of the control strategy also maintains operation at the optimal stall attack angle of 15^o [6]. Thus, the control strategy for a cyclorotor must satisfy two criteria: maximise the rotational velocity, and optimise attack angles.

In the next example we consider a constant rotational rate $\tilde{\omega} = \dot{\theta}/\omega$ and develop a optimal pitch control strategy for the same monochromatic wave (T = 10 s and H = 2 m) using the representation of (16). Fig. 7 illustrates the recommended optimal pitch angles for the case of cyclorotors, with one and two hydrofoils, within one wave period.

As can be seen from Fig. 8, real-time pitch control results in a very modest increase in mechanical power (for this monochromatic case), with convergence achieved after m = 3-5 harmonics. However, it can be concluded that variational pitch control is more effective for the single-foil rotor than the twin-foil case. Nevertheless, the generated power for the single-foil cyclorotor, with variable pitch, does not exceed the power generated by a twin-foil cyclorotor rotating with constant velocity and optimal *constant* pitch angles.

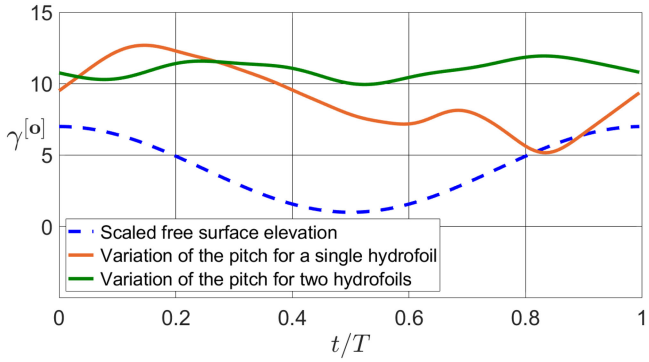

Fig. 7. Pitch angle variations, within a wave period, obtained for the case of the single hydrofoil (orange line, $m = 12$) and two hydrofoils (green line, $m = 12$), for an optimal constant rotational rate. The scaled free surface elevation is presented for reference.

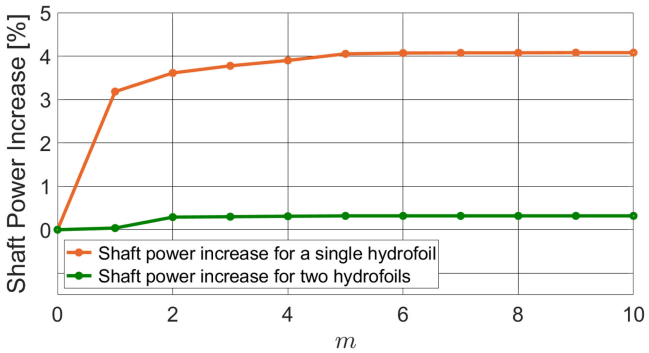

Fig. 8. The increase in cyclorotor performance with the number of harmonics, for the solution for variable pitch and optimal constant rotational rate.

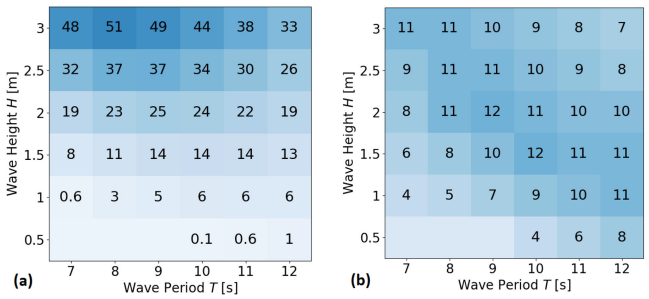

Fig. 9. (a) Mechanical power generation in [kW/m] for constant rotational rate with optimal constant pitch angles for various monochromatic waves. (b) Optimal constant pitch angle values in [deg].

Figs. 9 and 10 summarise the power capture performance increase for a twin-foil cyclorotor with the specified real-time control strategies, for various monochromatic waves. First, we evaluate the generated mechanical power Fig. 9(a), for a constant rotational rate $\dot{\theta} = \omega$ and define the corresponding optimal constant pitch angle values $\gamma_1 = -\gamma_2$ Fig. 9(b), for a variety of wave heights H and periods T of incoming monochromatic waves. The performance values presented in Fig. 9(a) will be used as a reference to asses the power increase caused by real-time control.

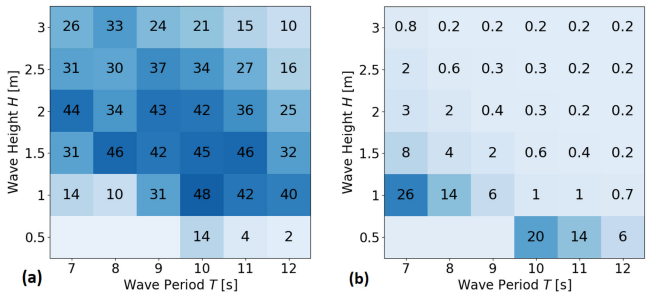

Fig. 10. Percentage increase in rotor power performance after implementation of the optimal control for various monochromatic waves. (a) Variable rotational rate and optimal constant pitch. (b) Constant rotational rate and variable pitch.

It can be seen, from Fig. 10(a), that an optimal (variable) rotational rate increases the shaft power by an average of 30%. It is also noticeable that the increase in the generated power has a nonlinear dependence on the height H and period T of the monochromatic wave. This nonlinear dependence can be explained by the significant nonlinearity of the functional in (14).

Variable pitch angle control does not significantly increase the generated power for most of the cells in Fig. 10(b). This strategy is productive only in the case of waves with a short period and small height; however, the absolute value of the power generated for these waves is not very significant, as shown in Fig. 9(a).

The obtained results illustrate that the control of rotational rate in monochromatic waves can significantly increase the generated shaft power P_{Shaft}. In contrast, active pitch control in monochromatic waves does not significantly increase the shaft power P_{Shaft}, suggesting the use of an optimal constant pitch angle, for monochromatic waves, especially considering the additional complexity of underwater pitch actuators.

IV. Optimal Real-Time Control Solutions for Panchromatic Waves

In this section, we present the results of the application of the spectral solution forms of (17), (18), and (19) to the optimal pitch and/or rotational rate control problems for a cyclorotor with two hydrofoils, in panchromatic waves. We use one of the 2D structural (submergence depth and rotor radius) cyclorotor designs which were proposed by the LiftWEC consortium [2], [20], for the most frequent sea state $T_e = 8\,s$ and $H_s = 1.5\,m$ of the south-west coast of Brittany (Audierne Bay 47.84° N, 4.83° W) [38]:

$$R = 8m,\ C = 6.4m,\ y_0 = -11.25m,\ \gamma_0 = 0^o \qquad (21)$$

which can produce, on average, $P_{Shaft} = 658 \pm 7\,W/m$ if it switches between optimal constant rotational rates for different sea-states (T_e, H_s). The moment of inertia I of the cyclorotor, which plays a role in the panchromatic case, is proportional to its radius R and chord length C and the following approximation:

$$I = 2\,R^2\,C\,M \qquad (22)$$

where $M = 2kg/m^2$ is the mass of one square metre of foil surface, is employed. The same shaft torque $\mathcal{T}$ limitations, as in Section III, are employed.

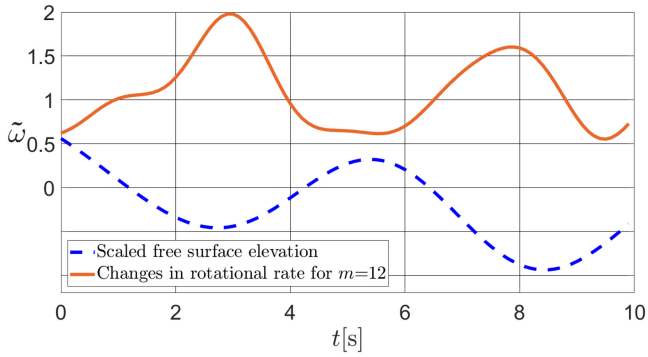

Fig. 11. The change in rotational rate $\tilde{\omega}$ during a 10 s panchromatic wave realisation (in red), and the wave profile (in blue). A neutral constant pitch angle is used, i.e. $\gamma_i = 0$.

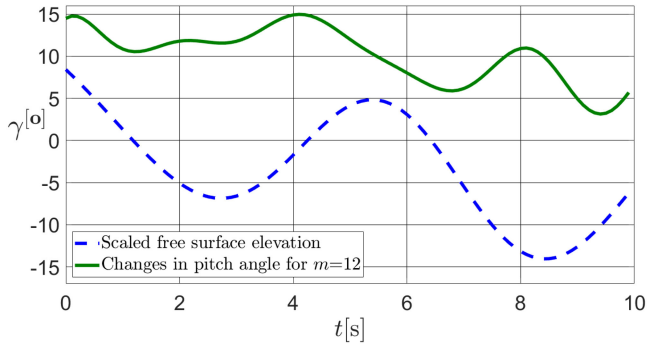

Fig. 12. The variable pitch profile (in green) during a 10 s panchromatic wave realisation, and the corresponding free surface elevation (in blue). Optimal constant velocity is used $\dot{\theta}_0 = 0.22\,rad/s$.

Control is initiated after $T_0 = 40$ s, allowing the formation of a fluid particle velocity field in the vicinity of the rotor. It is assumed, for the purpose of this fundamental control study, that we know all characteristics of the incoming wave package within the next $T - T_0 = 10$ s time interval. In a more realistic scenario, some estimation/forecasting techniques need to be employed [3], [39], [40]. The period $T_{ext} = 20$ s of the series (18), and (19) exceeds $T - T_0 = 10$ s interval, permitting the optimal position, rotational rate and values of the pitch angles, at the start of the generated power calculation, to be achieved.

A. Optimal Control Solution for a Variable Rotational Rate

A solution for the optimal variable rotational rate, with constant neutral pitch, in 10 s realisations of panchromatic waves (17), (18), and the corresponding convergence assessment, are presented in Figs. 11 and 14, respectively. The constant rotational rate ($m = 0$) for the selected interval was evaluated as $\dot{\theta}_0 = 0.22\,rad/s$, and is used to normalise the variable rotational rate $\dot{\theta}$: $\tilde{\omega} = \dot{\theta}/\dot{\theta}_0$ and implement the constraint $1/2 < \tilde{\omega} < 2$ on the rotational rate for the search of the next m harmonics.

Fig. 12 shows the optimal changes in rotational rate, with the (scaled) free surface elevation above the rotor centre provided for reference. Note the correlation between curves, demonstrating acceleration of the rotational rate at the moments of decreasing free surface elevation, and deceleration with increases free

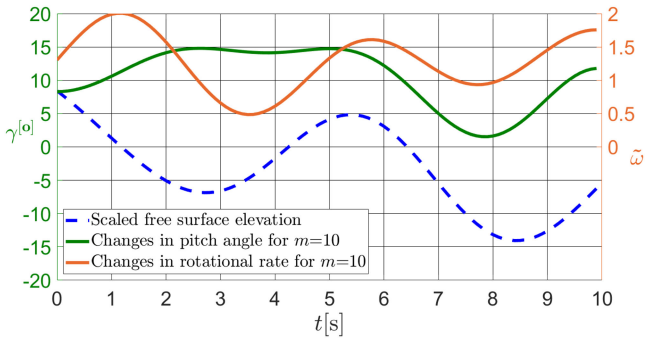

Fig. 13. The change in pitch angle (in green) and rotational rate (in red) during 10 seconds interval of panchromatic waves, and the wave profile (in blue).

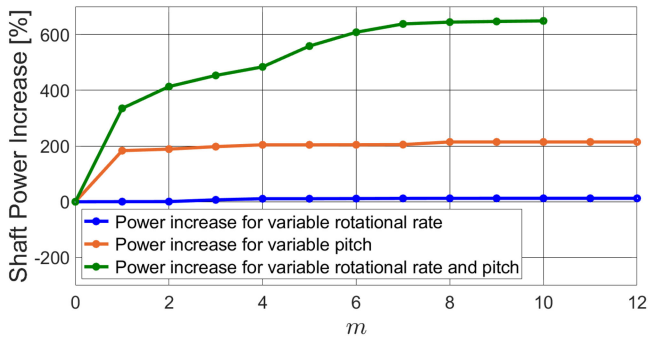

Fig. 14. The increase in rotor performance with increasing number of solution harmonics for variable pitch angle and/or variable rotational rate, for various control strategies presented on Figs. 11–13.

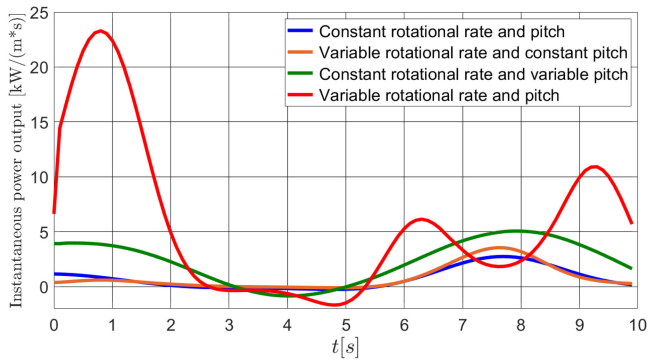

Fig. 15. The instantaneous power output under different control strategies [kW/(m*s)], for various control strategies presented in Figs. 11–13.

surface elevation. Convergence of the variable rotational rate solution is achieved after $m = 6$ harmonics, as shown in Fig. 14. The originally estimated shaft power value $P_{Shaft} = 738.47$ W/m, for the constant optimal rotational rate $\dot{\theta}_0$ and neutral pitch $\gamma_0 = 0^o$, increases to $P_{Shaft} = 883.81$ W/m, with optimal rotational rate control. Six realisations of panchromatic waves with ($H_s = 1.5$ m and $T_e = 8$ s) show an average increase in the absorbed mechanical power of 10–40%, over the constant rotational rate case, and it can be noted that the performance increase is generally greater then the corresponding average power increase for the case of monochromatic waves. Crucially for the panchromatic wave case (17), we also use the moment

TABLE I
PERFORMANCE (W/M), IN TERMS OF SHAFT POWER P_{Shaft}, FOR SIX DIFFERENT PANCHROMATIC WAVE REALISATIONS (Nº)

Nº	Constant $\dot{\theta}$ Constant γ	Variable $\dot{\theta}$ Constant γ	Constant $\dot{\theta}$ Variable γ	Variable $\dot{\theta}$ Variable γ
1	738.47	883.81	2322.57	5684.36
2	640.82	656.03	2771.36	6119.96
3	155.55	241.36	427.16	1346.15
4	628.74	689.42	2770.08	6061.03
5	382.65	572.7	947.09	1809.53
6	435.36	540.82	1612.4	4816.83

of inertia of the rotor I, which may be beneficial for power increase. Equally, exceptionally large values of rotor inertia may slow real-time control actions and cause significant undesirable structural loads.

B. Optimal Control Solution for a Variable Pitch Angle

Results obtained for optimal pitch control (17), (19), with an optimal constant rotational rate $\dot{\theta}_0 = 0.22\,rad/s$, generally show more than a 200% increase in the generated power. Such a significant increase in the shaft power for optimal pitch control is in agreement with results obtained in Section III, which show that the tuned constant pitch angle can increase power production by more than 100%, in comparison with a constant neutral pitch of 0^o, for monochromatic waves.

Thus, for the variable pitch example presented in Fig. 12, $P_{Shaft} = 2322.12$ W/m for the same panchromatic wave input as Fig. 11. This is an almost 200% increase in generated power in comparison with the results obtained for the optimal constant rotational rate and neutral pitch angle. Eight harmonics ($m = 8$) are sufficient to achieve convergence of the solution in terms of the shaft power (Fig. 14).

C. Optimal Control Solution for Variable Velocity and Pitch

Finally, the combination of optimal rotational rate and pitch control (17), (18), (19) is examined, for the same 10 s interval of panchromatic waves ($H_s = 1.5$ m and $T_e = 8$ s). Fig. 13 illustrates the variations in rotational rate and pitch angle. The combined control strategy returns $P_{Shaft} = 5684.36$ W/m, also showing an average increase in power absorption value estimated for the fixed pitch and rotational rate, of factor 7–9, using a range of sea state realisations (see Table I).

Fig. 13 also show the correlation between free surface elevation and the optimal variations in rotational rate and pitch angle. Eight solution harmonics ($m = 8$) harmonics, for both variable rotational rate and variable pitch angle, are sufficient to achieve convergence, as shown in Fig. 14.

D. Discussion of the Optimal Control Strategies

In our research, we consider only short 10 s intervals. The increase of the time interval will require a significant increase in the number of required series coefficients, which greatly increases the calculation time, due to the nonlinearity of the problem. To confirm the statistical significance of the results, a table of the performance increase, for the various control

strategies for six different short panchromatic waves realisations, is presented in Table I.

The significant power increase for the case of joint control (Table I, Fig. 15) can be explained by the fact that only with the use of both actuators can we satisfy both conditions of generated mechanical power maximisation: maintaining optimal stall attack angle at all times [6] and having the maximum possible rotational rate for the current conditions. It is clear that full exploitation of the tangential force (10) caused by the interaction between foils and wave induced water particles will require permanent tuning/real time control of the hydrofoils; otherwise, the performance of the device will be modest.

The performance of the rotor, in terms of mechanical power P_{Shaft}, is not closely connected to the incoming wave power P_{Wave}. However, the obtained mechanical power generation P_{Shaft} presented for the joint control strategy (see Table I) are close to the averaged wave power $P_{Wave} = 8.3\,kW/m$ for a panchromatic wave with state $T_e = 8\,s$ and $H_s = 1.5\,m$. It can be indirectly confirmed, by the numerical and experimental assessments conducted by the Atargis [1], [6], that cyclorotor-based WECs can entirely cancel the incoming wave by completely absorbing its energy.

V. Conclusion

The research conducted in the article has clearly shown the benefits of the optimal pitch and rotational rate control application, in both monochromatic and panchromatic waves. While rotational rate control looks more compelling than pitch control, in terms of shaft power increase in monochromatic waves, this observation is reversed in the case of panchromatic waves. The implementation of the joint pitch and rotational rate control strategy in panchromatic waves shows a significant increase over the fixed or single input of rotational rate/pitch cases. The main conclusion from the presented results, therefore, is that cyclorotors must be controlled in real time using both actuators, in order to reach their full potential.

In general, just 8-9 harmonics for the optimal solution for rotational rate and/or pitch angles are shown to be sufficient, giving significant increase in the generated power (Fig. 14). This relatively small number of coefficients which must be determined for an acceptable solution, allow for efficient computer implementation, while the use of a relatively small number of harmonics maintains smooth profiles for the operational variables (torque, velocity, etc), minimising detrimental cyclical and extreme loading on system components.

A limitation of this study is the use of perfect information, in relation to the incoming wave, in the determination of the optimal solutions for foil pitch and rotational rate. Real time implementation, which will require significant further development, in terms of computation, local servo loops, receding horizon formulation, and estimation/forecasting (see, for example, [21], [39], [40]), are considered to be beyond the scope of the current study.

Nevertheless, the conducted research has shown that advanced control of cyclorotor-based WECs has significant potential and requires further analytical, numerical, and experimental study.

References

[1] Atargis, the Energy Corporation, 2021, Accessed: Mar. 10, 2022. [Online]. Available: https://atargis.com//

[2] LiftWEC Consortium, 2021, Accessed: Mar. 10, 2022. [Online]. Available: https://liftwec.com/

[3] C. Fagley, A. Mohtat, K. Chitale, and S. Siegel, "Dynamic estimation and control of a cycloidal wave energy converter in three-dimensional sea states," in *Proc. 14th Eur. Wave Tidal Energy Conf.*, 2021, Art. no. 2120.

[4] A. Mohtat, C. Fagley, K. C. Chitale, and S. G. Siegel, "Efficiency analysis of the cycloidal wave energy convertor under real-time dynamic control using a 3D radiation model," in *Proc. 14th Eur. Wave Tidal Energy Conf.*, 2021, Art. no. 2144.

[5] K. C. Chitale, C. Fagley, A. Mohtat, and S. G. Siegel, "Numerical evaluation of climate scatter performance of a cycloidal wave energy converter," in *Proc. 14th Eur. Wave Tidal Energy Conf.*, 2021, Art. no. 2141.

[6] S. G. Siegel, "Numerical benchmarking study of a cycloidal wave energy converter," *Renew. Energy*, vol. 134, pp. 390–405, 2019.

[7] M. Folley and T. Whittaker, "Lift-based wave energy converters - an analysis of their potential," in *Proc. 13th Eur. Wave Tidal Energy Conf.*, 2021, Art. no. 1446.

[8] A. Ermakov and J. V. Ringwood, "Rotors for wave energy conversion-practice and possibilities," *IET Renew. Power Gener.*, vol. 15, pp. 3091–3108, 2021.

[9] A. Hermans, E. Van Sabben, and J. Pinkster, "A device to extract energy from water waves," *Appl. Ocean Res.*, vol. 12, no. 4, pp. 175–179, 1990.

[10] J. Pinkster and A. Hermans, "A rotating wing for the generation of energy from waves," in *Proc. 22nd Int. Workshop Water Waves Floating Bodies*, 2007, pp. 165–168.

[11] C. P. Fagley, J. J. Seidel, and S. G. Siegel, "Computational investigation of irregular wave cancellation using a cycloidal wave energy converter," in *Proc. Int. Conf. Offshore Mechanics Arctic Eng.*, 2012, pp. 351–358.

[12] S. G. Siegel, C. Fagley, M. Römer, and T. McLaughlin, "Experimental investigation of irregular wave cancellation using a cycloidal wave energy converter," in *Proc. Int. Conf. Offshore Mechanics Arctic Eng.*, 2012, pp. 309–320.

[13] S. Siegel, C. Fagley, and S. Nowlin, "Experimental wave termination in a 2D wave tunnel using a cycloidal wave energy converter," *Appl. Ocean Res.*, vol. 38, pp. 92–99, 2012.

[14] C. P. Fagley, J. J. Seidel, and S. G. Siegel, "Wave cancellation experiments using a 1:10 scale cycloidal wave energy converter," in *Proc. 1st Asian Wave Tidal Energy Conf.*, 2012, pp. 27–30.

[15] S. G. Siegel, "Cycloidal wave energy converter," Federal Agency to which Report is submitted: DOE EERE - Wind and Water Power Program, Atargis Energy Corporation, Pueblo, CO, USA, Final Sci. Rep.: DOE/EE0003635, 2013.

[16] N. Scharmann, "Ocean energy conversion systems: The wave hydro-mechanical rotary energy converter," Ph.D. dissertation, Inst. Fluid Dyn. Ship Theory, TUHH, Hamburg, Germany, 2014.

[17] J. Chozas, A. Tetu, and A. Arredondo-Galeana, "A parametric cost model for the initial techno-economic assessment of lift-force based wave energy converters," in *Proc. 14th Eur. Wave Tidal Energy Conf.*, 2021, Art. no. 2005.

[18] M. Folley and P. Lamont-Kane, "Optimum wave regime for lift-based wave energy converters," in *Proc. 14th Eur. Wave Tidal Energy Conf.*,2021, Art. no. 1914.

[19] P. Lamont-Kane, M. Folley, C. Frost, and T. Whittaker, "Preliminary investigations into the hydrodynamic performance of lift based WECs," in *Proc. 14th Eur. Wave Tidal Energy Conf.*, 2021, Art. no. 2074.

[20] J. V. Ringwood and A. Ermakov, "Energy-maximising control philosophy for a cyclorotor wave energy device," in *Proc. 41st Int. Conf. Ocean, Offshore Arctic Eng.*, Art. no. 80990.

[21] L. Wang, J. Isberg, and E. Tedeschi, "Review of control strategies for wave energy conversion systems and their validation: The wave-to-wire approach," *Renew. Sustain. Energy Rev.*, vol. 81, pp. 366–379, 2018.

[22] A. Ermakov and J. V. Ringwood, "A control-orientated analytical model for a cyclorotor wave energy device with n hydrofoils," *J. Ocean Eng. Mar. Energy*, vol. 7, pp. 201–210, 2021.

[23] A. M. Ermakov and J. V. Ringwood, "Erratum to: A control-orientated analytical model for a cyclorotor wave energy device with N hydrofoils," *J. Ocean Eng. Mar. Energy*, vol. 7, pp. 493–494, 2021.

[24] A. Ermakov and J. V. Ringwood, "Development of an analytical model for a cyclorotor wave energy device," in *Proc. 14th Eur. Wave Tidal Energy Conf.*, 2021, Art. no. 1885.

[25] A. Arredondo-Galeana *et al.*, "A methodology for the structural design of LiftWEC: A wave-bladed cyclorotor," in *Proc. 14th Eur. Wave Tidal Energy Conf.*, 2021, Art. no. 1967.

[26] A. Ermakov *et al.*, "LiftWEC project deliverable D5.2 validated numerical model with real-time computational capabilities," 2021, Accessed: Mar. 10, 2022. [Online]. Available: https://liftwec.com/

[27] G. Olbert *et al.*, "LiftWEC project deliverable D3.3: Tool validation and extension report," 2021, Accessed: Mar. 10, 2022. [Online]. Available: https://liftwec.com/

[28] H. G. Dawson, "On the numerical value of $\int_0^h e^{x^2}\,dx$," *Proc. London Math. Soc.*, vol. s1-29, no. 1, pp. 519–522, 1897.

[29] G. K. Batchelor, *An Introduction to Fluid Dynamics*. Cambridge, U.K.: Cambridge Univ. Press, 1967.

[30] G. Bacelli and J. V. Ringwood, "Numerical optimal control of wave energy converters," *IEEE Trans. Sustain. Energy*, vol. 6, no. 2, pp. 294–302, Apr. 2015.

[31] N. Faedo, G. Scarciotti, A. Astolfi, and J. V. Ringwood, "Energy maximising control of wave energy devices using a moment-domain representation," *Control Eng. Pract.*, vol. 81, pp. 85–96, 2018.

[32] Scipy.org, "Python optimisation library," 2021, Accessed: Mar. 10, 2022. [Online]. Available: https://docs.scipy.org/doc/scipy/reference/optimize.html

[33] A. Iserles, *A First Course in the Numerical Analysis of Differential Equations*. New York, NY, USA: Cambridge Univ. Press, 2009.

[34] S. Endres, C. Sandrock, and W. Focke, "A simplicial homology algorithm for Lipschitz optimisation," *J. Glob. Optim.*, vol. 72, pp. 181–217, 2018.

[35] R. Storn and K. Price, "Differential evolution - A simple and efficient heuristic for global optimization over continuous spaces," *J. Glob. Optim.*, vol. 11, pp. 341–359, 1997.

[36] R. Sheldahl and P. Klimas, "Aerodynamic characteristics of seven symmetrical airfoil sections through 180-degree angle of attack for use in aerodynamic analysis of vertical axis wind turbines," Sandia Nat. Labs., Albuquerque, NM, USA, Tech. Rep. SAND-80-2114, 1981.

[37] G. Giorgi and J. V. Ringwood, "Implementation of latching control in a numerical wave tank with regular waves," *J. Ocean Eng. Mar. Energy*, vol. 2, no. 2, pp. 211–226, 2016.

[38] E. Boudière, C. Maisondieu, F. Ardhuin, M. Accensi, L. Pineau-Guillou, and J. Lepesqueur, "A suitable metocean hindcast database for the design of marine energy converters," *Int. J. Mar. Energy*, vol. 3/4, pp. 40–52, 2013.

[39] Y. Peña-Sanchez, C. Windt, J. Davidson, and J. V. Ringwood, "A critical comparison of excitation force estimators for wave-energy devices," *IEEE Trans. Control Syst. Technol.*, vol. 28, no. 6, pp. 2263–2275, Nov. 2020.

[40] Y. Pena-Sanchez, A. Mérigaud, and J. V. Ringwood, "Short-term forecasting of sea surface elevation for wave energy applications: The autoregressive model revisited," *IEEE J. Ocean. Eng.*, vol. 45, no. 2, pp. 462–471, Apr. 2020.